# Sharpening methods for low-contrast images based on nonlocal differences

## Métodos de mejora de nitidez para imágenes de bajo contraste basadas en diferencias no locales

**Yan Chen[1,2], Quan Zhang[1] and Zhiguo Gui[1]**

[1] Shanxi Provincial Key Laboratory for Biomedical Imaging and Big Data, North University of China, Xueyuan Road 3#, Taiyuan, 030051, Shanxi, China
[2] School of Engineering and Computer, Oakland University, 2200 N. Squirrel Road, Rochester, 48309-4401, Michigan, U.S.A

**DOI: http://dx.doi.org/10.6036/9315** | Recibido: 24/06/2019 • Inicio Evaluación: 24/06/2019 • Aceptado: 06/09/2019

## RESUMEN

Varios fenómenos, tales como el ruido cuántico y la dispersión, existentes en el proceso de obtención de imágenes con rayos X industriales, así como la complejidad estructural de la pieza radiografiada, pueden dar como resultado imágenes de rayos X industriales borrosas y de bajo contraste, lo que origina dificultades en el análisis de las imágenes de rayos X. Este estudio propuso un algoritmo mejorado de ajuste adaptativo para aumentar el contraste y la calidad de estas imágenes de rayos X. Se estableció una relación de características no locales entre los píxeles de la imagen y el entorno por medio de un modelo de filtrado no local basado en el modelo de medición del índice de similitud estructural (SSIM). Se calculó la semejanza estructural de los píxeles basados en bloque en el área de la ventana de búsqueda. El peso mejorado se combinó con el enfoque de la imagen resultando una gran mejora. La capacidad del algoritmo para conservar los bordes se verificó mediante pruebas de imagen. Finalmente, el algoritmo propuesto contribuyó a mejorar la calidad del contraste de las imágenes mediante experimentos de simulación. Los resultados demuestran que las características en diferencias no locales basadas en zonas anexas reflejan ricos detalles de las imágenes. Las imágenes de rayos X, de mayor nitidez con el algoritmo propuesto se caracterizan por sus excelentes efectos visuales y sus ricos detalles, con valores de entropía de información (IE) de 2,1464, 4,2453 y 3,7283 y similitudes estructurales de 0,9521, 0,9238 y 0,9534. Los pesos calculados por el SSIM indican que existe una gran similitud estructural entre la imagen nítida y la original. Las imágenes procesadas por el algoritmo de contrastado basado en diferencias no locales presentan detalles valiosos, a la vez que mantienen eficazmente los valores de los parámetros objetivos. Este estudio proporciona referencias para mejorar la calidad de las imágenes de bajo contraste.

• **Palabras clave:** no local, SSIM (medida del índice de similitud estructural), nitidez, bajo contraste.

## ABSTRACT

Various phenomena, such as quantum noise and scattering, existing in the industrial X-ray imaging process, and structural complexity of the measured workpiece resulted in low-contrast and blurry industrial X-ray images, which caused interference to the X-ray image analysis. This study proposed an improved adaptive sharpening algorithm to enhance the contrast and quality of X-ray images. Image pixels and the neighborhood established a non-local feature relationship through non-local filtering model on the basis of the structural similarity index measure (SSIM) model. The structural similarity of block-based pixels within the search window area was calculated. The improved weight was combined with image sharpening with high-enhancement results. The edge-preserving ability of the algorithm was verified through image tests. Finally, the proposed algorithm contributed to improving the quality of the contrast of industrial X-ray images through simulation experiments. Results demonstrate that features in the neighborhood based on non-local differences reflect rich details of images. The X-ray images sharpened with the proposed algorithm are characterized with excellent visual effects and rich details, with information entropy (IE) values of 2.1464, 4.2453, and 3.7283 and structural similarities of 0.9521, 0.9238, and 0.9534. The weights calculated by SSIM indicate that a high similarity in structure exists between the sharpened image and the original one. Images processed by the sharpening algorithm based on non-local differences present prominent details while effectively maintaining the objective parameter values. This study provides references to improve the quality of low-contrast images.

**Key words:** non-local, SSIM (structural similarity index measure), sharpening, low contrast.

## 1. INTRODUCTION

The common problems during the industrial X-ray imaging lie in the low contrast, narrow distribution of histogram, and lack of layering, which make it difficult to identify important details of X-ray images. On this basis, several researchers have conducted studies on the contrast enhancement of X-ray images [1-7].Large differences in the structure of industrial components and in the feature of details induced that the existing detection modes failed to solve problems related to feature extraction of all the images. Consequently, the preceding above analysis indicates that an effective sharpening model must be established, the image contrast must be increased, and the component details must be highlighted.

Therefore, this study proposed a filtering method on the basis of non-local differences to improve the contrast of X-ray images. The structural similarity of block-based pixels within the search window area was then measured to locate the edges and image details. A sharpening mask with high frequency was also constructed. The new sharpening algorithm was used to suppress noise while detecting image details for considering the structural details and non-local information of images.

## 2. STATE OF THE ART

Technologies related to digital image processing of workpieces have also become a major topic in the field of nondestructive testing. Many researchers worldwide have conducted studies on X-ray image detection. In 1978, Mian et al. of Japan proposed to use the least squares for fitting and then subtract the original image from the fitted one to remove the background and extract defects [8]. Echelt et al. believed that removing the high frequency in the image of the component through different low-pass filters and keeping the low frequency in the image are conducive to achieving image background simulation and defect extraction and segmentation [9]. These methods, however, lead to data loss in the fitting simulation process. Alasnanda proposed a detection algorithm for weld defects on the basis of morphology[10]. However, the capability of this method for detecting the fine line information is obscured. Daum et al. suggested the use of cubic spline curve fitting method to initially draw the background of welding image, an appropriate threshold is then selected to complete the defect extraction and segmentation [11]. However, such algorithm is time-consuming. Felisiberto et al. determined reasonable parameter values by using empirical threshold[12], the algorithm threshold needs to be empirically obtained. Mahmoudi et al. used a homomorphic filter to initially preprocess the image and then employed a global threshold method to extract the detailed information on the entire image. Such method exerts a less evident extraction for defects with complex shapes [13]. Yin and Su et al. reconstructed the background of welding by independent component analysis and then subtracted the background to extract the defects using OTSU [14]. The algorithm is strict in terms of image inputting. Chen and Ma et al. Preprocessed an image with median filtering for noise reduction, strengthened the transformation with high frequency, and extracted defects in the image with combination of the Inter-class and intra-class variance ratios [15]. Accordingly,Information loss still exists even though histogram equalization processing is adopted. Zhang et al. realized defect detection and extraction by watershed and Beamlet transforms, respectively [16].The results of image detection with background blur are biased by the algorithm. Deviation is observed for the detection result of images with fuzzy background. Y. Sun and H. Sun proposed a fuzzy recognition algorithm that can effectively segment the defects in the weld on the basis of image space [17]. In fuzzy recognition algorithms, every pixel is traversed, and processing for large industrial components is time-consuming. Shao and Du et al. proposed background removal and waveform analysis methods with double threshold to segment image in the welds, the methods have fine real-time performance and meet the requirements of video detection [18]. Zhang et al. detected the edge of the weld seam through a multiscale product and the entire image using sparse self-coding network [19]. The selection of algorithm parameters has a great influence on the results. Wang and Gao et al. conducted the principal component analysis for the matrix of identified circular defects and linearity of the image with fuzzy clustering method [20]. The algorithm needs to further optimize feature extraction to improve operation accuracy. Shao and Du et al. simulated the background of weld seams by using large-scale means filtering and extracted the slender defects in an image by Hough transform defect segmentation algorithm [21]. The proposed algorithm aims to process the local features of pixels without considering the non-local ones.

Methods concerning sharpening have been extensively studied in image enhancement[22-28].On this basis, the required details are usually contained in the high-frequency components of images. Unsharpening masks have been widely applied to improve image clarity. However, such method can possibly lead to overshoot during sharpening [29-30].

Non-local means processing has also become a method for image processing in recent years. The Non-local means algorithm was first raised by Buades et al. [31] in 2005 and applied to image denoising. Liu et al [32] proposed a new image denoising algorithm on the basis of the Non-local means and Laplace pyramid algorithms, which signifies that the robustness of the algorithm experience a significant improvement. Chatterjee et al. [33] extended the Non-local means algorithm to high-order kernel regression to achieve enhanced denoising on texture regions in the image. Other improvements or extensions of Non-local means algorithm have also achieved good results, such as the application of Non-local means filtering to SAR image denoising [34-35], improved Non-local means image denoising method that fully utilizes residual image information, and moment-based improved algorithm [36-38].

Wavelet transform has time-frequency characteristics, which can reflect local characteristics in both time and frequency domains[39-40]. It can be applied to image processing to achieve a variety of image processing. Wavelet transforms have been used for image contrast enhancement to take advantage of the multiscale properties in the wavelet domain[41].

A growing interest has been recently observed on sparse representations using dictionary learning (DL),Despite the successes of Sparse Representation techniques, a large number of dictionary atoms as well as the high dimension of the data can make these classifiers computationally demanding[42-43].Furthermore, sparse classifiers are subject to the adverse effects of a phenomenon known as coefficient contamination, where, for example, variations in pose may affect identity and expression recognition.

The present study adopted a Non-local means filtering model in handling the grayscale and position of the pixels in the neighborhood in different areas. The structural similarity of block-based pixels with multiplication of parameters was also improved on the basis of the structural similarity index measure (SSIM) model and algorithm of sharpening mask. Accordingly, the denoising effect of the algorithm in the structural edge region was enhanced. Lastly, the weight was integrated into the Laplacian sharpening algorithm with high enhancement, which provided a basis for the denoising and detail-preserving methods of low-contrast images.

The remainder of this study is organized as follows. Section 3 expounds the methods of extraction of feature and the design of new sharping method. Section 4 presents the experimental designs and analysis of results. Section 5 presents the summary and relevant conclusions of this study.

## 3. METHOD

### 3.1. FEATURE EXTRACTION

An image exhibits two features, namely, edge structure and texture. Selection of an appropriate method for edge feature extraction is conducive for analyzing and determining the contents of images. In addition, feature extraction selection also helps in understanding the contents when analyzing and assessing industrial X-ray images.

#### 3.1.1. Non-local feature extraction

Non-local means filtering theory stipulates that the value $\hat{f}(p_{ij})$ for a pixel $p_{ij}$ in a noisy image, which is processed by Non-

local means filtering[38], is expressed as follows:

$$\hat{f}(p_{ij}) = \sum_{p_{i'j'} \in S_{p_{ij}}} w(p_{ij}, p_{i'j'}) f(p_{i'j'}) \quad (1)$$

Such algorithm is novel in the calculation method of the weight coefficient $w(p_{ij}, p_{i'j'})$. The basic principle of the Non-local means algorithm for filtering is explained in Fig. 1. $f = \{f(p_{ij}) \mid i \in I, j \in J\}$ represents images that are contaminated by noise and are to be processed. The area $S_{p_{ij}}$ is marked as the search window and contains pixels and points in the neighborhood. Meanwhile, areas $M_{p_{ij}}$ and $M_{p_{i'j'}}$ are marked as the matching windows and refer to ranges that are centered on pixel $p_{ij}$ and neighboring pixel $p_{i'j'}$, respectively. $w(p_{ij}, p_{i'j'})$ indicates the weight coefficient between $p_{ij}$ and $p_{i'j'}$ pixels.

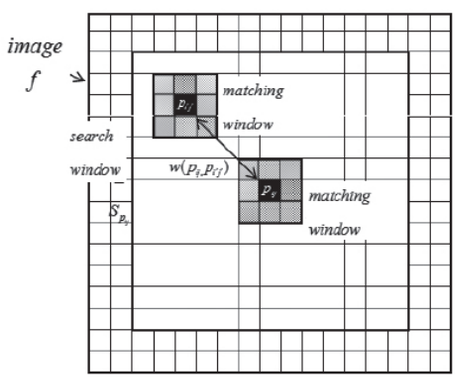


*Fig. 1: Schematic of the principle of Non-local means algorithm*

The calculation method is listed as follows:

$$w(p_{ij}, p_{i'j'}) = \frac{1}{Z(p_{ij})} e^{\frac{\left\| f(M_{p_{ij}}) - f(M_{p_{i'j'}}) \right\|_{2,a}^2}{h^2}},$$
$$0 \le w(p_{ij}, p_{i'j'}) \le 1, \quad \sum_{p_{i'j'} \in S_{p_{ij}}} w(p_{ij}, p_{i'j'}) = 1, \quad (2)$$
$$Z(p_{ij}) = \sum_{p_{i'j'} \in S_{p_{ij}}} e^{\frac{\left\| f(M_{p_{ij}}) - f(M_{p_{i'j'}}) \right\|_{2,a}^2}{h^2}}.$$

where $\|\cdot\|_{2,a}^2$ is the squared Euclidean distance weighted by Gauss. If $\alpha$>0, then the similarity measure of pixels $p_{ij}$ and $p_{i'j'}$ are standard deviations of the weighted Gaussian kernel. The degree of exponential attenuation is controlled by parameter $h$, whereas $Z(p_{ij})$ acts as normalization. The equations for $\|\cdot\|_{2,a}^2$ is as follows:

$$\left\| f(M_{p_{ij}}) - f(M_{p_{i'j'}}) \right\|_{2,a}^2 = \sum_k g_k (f_{p_{ij},k} - f_{p_{i'j'},k})^2. \quad (3)$$

As shown in Fig.1 and Equation (2), $\|\cdot\|_{2,a}^2$ does not simply refer to a single-point grayscale based on pixels $p_{ij}$ and $p_{i'j'}$ but to the neighborhood gray information based on the pixels in matching windows $M_{p_{ij}}$ and $M_{p_{i'j'}}$ and on the weight coefficients $g_k$ satisfying the 2D Gaussian distribution, considering the grayscale and location of pixels within the neighborhood.

The size of the window usually does not select the whole image to be filtered; the matching window radius are smaller than the search window radius, and the selection is based on the similarity of the window. The parameters controlling the exponential attenuation have a direct impact on the smoothness of the processed image. With the increase of the h value, the weight value of the pixels with low similarity increases correspondingly, which is reflected in the image processing effect that the smoothness degree increases and the edge tends to blur; on the contrary, the smoothness degree decreases, but it may cause poor denoising effect.

On the basis of the preceding principles, the main idea of Non-local means filtering can be summarized as follows. Additional pixels in the search window that are as similar as possible to the pixels to be filtered are explored to participate in the filtering process. Meanwhile, the similarity measure considers the grayscale and location of pixels in the matching window.

### 3.1.2. Measurement of structural similarity

Grayscale of pixels are applied to the traditional Non-local means filtering algorithm for calculating similarity among images. This approach certainly exerts limitations on the measurement structural similarity on account of the grayscale application as a similarity measure of small blocks. Non-local means filtering algorithm shows an excellent denoising effect on flat areas of the image. However, the effect is not evident in images where rich information is present. To solve this problem, an SSIM model is utilized as the similarity measure criterion between the two block-based pixels. This model, which is widely applied in objective evaluation on image quality, is a SSIM proposed by Zhou et al. [44]. SSIM is also a full reference model that combines luminance, contrast, and structural information of images. The SSIM model is shown in Fig. 2.

$$l(x,y) = \frac{2u_x u_y + c_1}{u_x^2 + u_y^2 + c_1}, \quad c(x,y) = \frac{2\delta_x \delta_y + c_2}{\delta_x^2 + \delta_y^2 + c_2}, \quad s(x,y) = \frac{\delta_{xy} + c_3}{\delta_x + \delta_y + c_3} \quad (4)$$

Comparison function for luminance:

$$l(x,y) = \frac{2u_x u_y + c_1}{u_x^2 + u_y^2 + c_2} \quad (5)$$

Comparison function for contrast:

$$c(x,y) = \frac{2\delta_x \delta_y + c_1}{\delta_x^2 + \delta_y^2 + c_2} \quad (6)$$

Comparison function for structure:

$$s(x,y) = \frac{\delta_{xy} + c_3}{\delta_x + \delta_y + c_3} \quad (7)$$

In the preceding equations, $u$ and $\delta$ indicate the mean and variance of the grayscale of a block-based image that is centered on pixel $x$, and $c_1$, $c_2$, and $c_3$ represent the minimal values that exclude zero division.

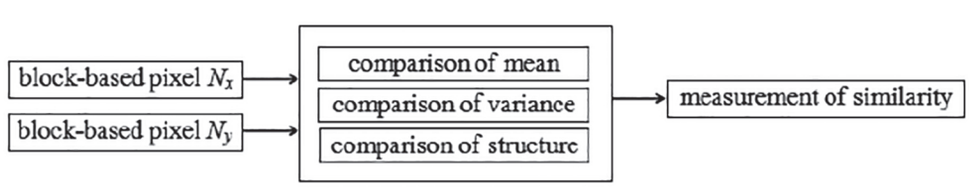


*Fig. 2: System diagram for SSIM model*

$$SSIM(x,y)=[l(x,y)]^{\alpha}[c(x,y)]^{\beta}[s(x,y)]^{\gamma} \quad (8)$$

When the absolute value of SSIM is large, the similarity between the two small blocks is good. The structural similarity parameters are defined to be consistent with the monotonicity of the Euclidean distance weighted by Gaussian, as shown as follows:

$$s(x,y)=\frac{1-SSIM(x,y)}{2} \quad (9)$$

The value interval is set as [0, 1]. When the absolute value of *s(x, y)* is large, the similarity between the two small block-based pixels is low. The same monotonicity as Euclidean distance weighted by Gauss lies in such notion. This study takes the multiplication of parameters based on the SSIM model and Euclidean distance weighted by the original Gauss as an improvement on the structural similarity of block-based pixels.A threshold t is set for *s(x, y)* to reduce the calculation time of the proposed algorithm. Only when the value of s(x, y) is greater than that of t will block-based pixels be added to the similar set of pixels, otherwise, its weight will be re-set to 0. The details are shown in the following equation:

$$W(x,y)=\begin{cases}\frac{1}{c(x)}e^{\frac{-d(x,y)}{h^2}}, & s(x,y)\geq t\\ 0, & s(x,y)<t\end{cases}. \quad (10)$$

The value of t is determined to be 0.2. When the value of *s(x, y)* is greater than 0.2, the searched similar block-based pixels will be useful,when it is less than 0.2, similar block-based pixels will be discarded out of low similarity.

$$d(x,y)=s(x,y)\left\|v(N_x)-v(N_y)\right\|_2^2 \quad (11)$$

It can be seen from formula 11 that the distance weights in non-local computation can be adaptively adjusted by calculating the similarity of matching windows.

## 3.2 SHARPENING ALGORITHM

### 3.2.1 High-enhancement sharpening mask

In view of the advantages of Non-local means algorithm, this study proposed a high-enhancement sharpening mask with combination of Non-local means filtering algorithm and image sharpening.

The sharpening mask used for sharpening is shown in Fig.3. Parameter A controls the degree of high enhancement, which is named as the high-enhancement parameter in this study.

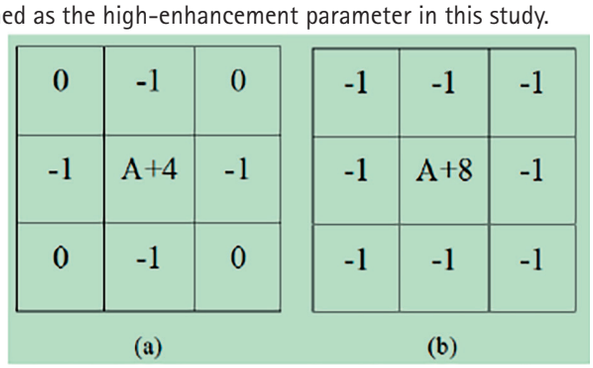


*Fig. 3: High-enhancement algorithm of sharpening mask (a) four-neighborhood form (b) eight-neighborhood form*

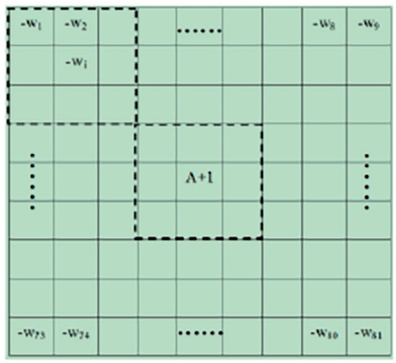


*Fig. 4: High-enhancement algorithm of sharpening mask proposed in this study*

The mask in Fig. 3(b) was extended in accordance with the Non-local mean filtering algorithm. A new high-enhancement sharpening mask was proposed in this study through coefficient value calculation by using the idea of the Non-local means algorithm.

In comparison with the classic mask shown in Fig.3, the mask shown in Fig.4 is novel because of the following reasons: (1) the size of the mask is increased and is variable, which corresponds to the search window in the non-local mean algorithm illustrated in Fig.1. (2) the fixed coefficient value in the classic mask is improved to $-w_i$ and $w_i$ is calculated in the method to calculate the weight value in the Non-local means filtering algorithm presented in Equation (2).

The two windows indicated by the dotted line in Fig.4 correspond to the matching window in Fig.1 and are used to calculate $w_i$.

### 3.2.2 Sharpening algorithm based on nonlocal differences

$f_{center}$ is used to represent the pixel value (grayscale) in the image to be enhanced at the center of the mask. In this way, the result processed by the high-enhancement sharpening algorithm based on the improved mask mentioned in Section 3.1.1 is expressed as follows:

$$\hat{f}_{center}=(A+1)f_{center}-\sum_i w_i f_i, \quad (12)$$

$$\hat{f}_{center}=\max(\hat{f}_{center},0),$$

$$\hat{f}_{center}=\min(\hat{f}_{center},255).$$

In Equation (12), $f_i$ is the pixel value in the corresponding mask $w_i$ in the image to be enhanced, and $\hat{f}_{center}$ is the corresponding enhancement result of $f_{center}$. Operations max and min limit the range of grayscale to between [0, 255].

It is displayed and processed the actual gray image that the gray value less than zero is assigned to 0, while the one greater than zero is addressed to 255. Specifically, the grayscale that is less than zero is assigned to 0, and that greater than zero is assigned to 255 to utilize the display and processing of the actual gray map. Given that the idea of nonlocal means filtering is introduced when calculating the coefficient $w_i$ in Equation (12), the algorithm described in this equation is called a sharpening algorithm based on nonlocal differences. When A=0 in Equation (12), $\hat{f}_{center}=f_{center}-\sum w_i f_i$, similar to the processing effect of Laplace operator, which is called nonlocal differences in this study.

The proposed algorithm in this study uses the theory of nonlocal means filtering, considers the structural details when calculating the coefficients, and uses the nonlocal information in the

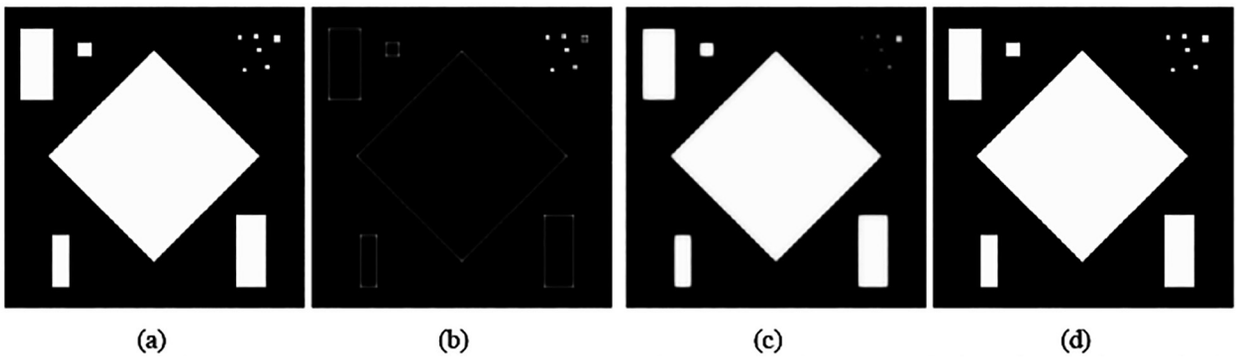


*Fig. 5: Test results of geometric composite image(a)original image (b) the proposed algorithm in this study (c) the proposed algorithm in this study when A=1 (d) differences between Figs.5(a) and 5(b)when A=0*

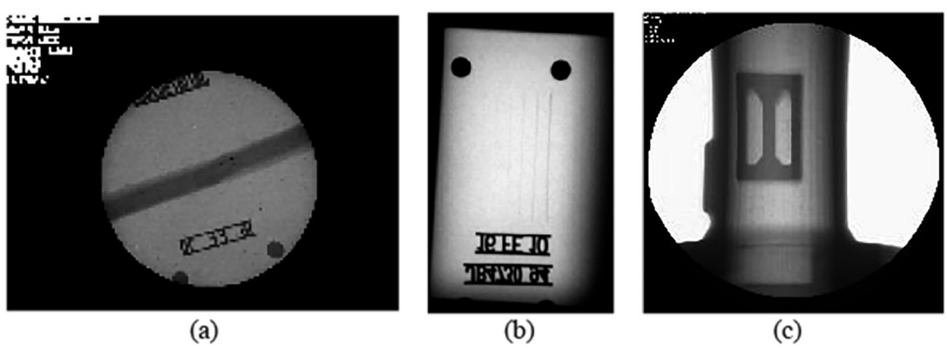


*Fig. 6: X-ray image(a)image of steel pipe weld(b)image of steel pipe weld(c)images of automotive Components*

image, thereby providing theoretical basis for improving the image enhancement effect. Geometric composite images are illustrated here to simply verify the effectiveness of the new algorithm, and additional relevant experiments will be described in detail in the subsequent contents of this chapter. During the test, two situations, that is, A=0 and A=1, are present in Equation (12). The test results are shown in Fig.5.

The geometrically composite original image and the processing result of the algorithm described in Equation (12) when A=0 are shown in Figs.5(a) and 5(b), respectively. In this case, the algorithm is characterized with an effect similar to that of Laplace algorithm for operator. The edge information of the original image is obtained in this figure. The edge information map shows that the edge information of the original image has been effectively extracted. The processing result of this algorithm when A=1 is shown in Fig.5(c). As shown in Equation (12), when A=1, the following expression is obtained:

$$\hat{f}_{center} = f_{center} + (f_{center} - \sum_i w_i f_i). \quad (13)$$

The first item at the right end of Equation (13) refers to the original image shown in Fig.5(a). The expression in brackets corresponds to the edge information shown in Fig.5(b). Therefore, Fig.5(c), which is the superposition of Figs.5(a) and 5(b), represents the enhanced results. Meanwhile, the difference between Figs.5(a) and 5(b) is shown in Fig.5(d). This subpanel indicates the residual graph after the original image is processed by the proposed algorithm when A=0 and also a set of blurred images when the edge information is separated from the original image. This effect is equivalent to that of the original image when processed through low-pass filtering, similar to the low-frequency component in wavelet transform. The comprehensive observation and analysis results for Fig.5 indicate that the edge information shown in Fig.5 (b) is clear and regular compared with the original image in Fig.5(a). The edge of the enhanced Fig.5(c) is clear and distinctive in terms of color, and Fig.5(d) shows a smooth and blurred edge due to the separation of high-frequency edge information. This finding also verifies the effectiveness of the algorithm in extracting high-frequency information. The results based on graphs indicate that the proposed algorithm in this study efficiently performs in edge preservation and image enhancement.

## 4. RESULT ANALYSIS AND DISCUSSION

In this section, experiments were performed for verification, and the influence of parameters in the algorithm on sharpening effects was conducted. Comparative analyses between different algorithms and the proposed algorithm in this study were also performed to evaluate the performance of image sharpening of the proposed algorithm.

Experimental software and hardware platforms include Intel (R) Core (TM) i5 3.10 GHz CPU with 4 GB memory, Windows 7 operating system, and Matlab 2016a as the programming platform.

The proposed algorithm was compared with the traditional contrast enhancement method in this section to intuitively analyze the advantages of the model suggested in this study, with the application of the image of industrial X-ray image for experimental tests.

The data used in this section are the actual X-ray image collected in the industrial field, as shown in Figure 6. The image size is 512 pixels by 512 pixels. The main acquisition parameters of the actual X-ray images are: voltage 120Kv, current 3.5m. In the experiments, We compared the performance of the proposed method with five methods, including the histogram equalization, Laplacian opreator,Top-hat,Wavelet,K-SVD.

In the proposed method,the size of the patch and the search window are 5×5 and 11×11, respectively. The filtering scale parameter *h* is associated with the noise standard deviation.

We use the image contrast to evaluate the quality of the sharped image. Assuming that *f* and *g* is the image gray value, *k* is the neighborhood of the pixel *f(i,j)*. The image contrast is employed to evaluate the the contrast between light and dark of the image. The bigger the contrast value, the stronger the image hierarchy and the higher the definition. Defined as

$$C = \sum_{k} (f(i,j) - g(i,j))^2 P_k(i,j) \tag{14}$$

Where $P_k(i,j)$ is the distribution probability of adjacent pixels in *k* neighborhood.

Figure 7-9 (material suplementario) show the results after applying the proposed algorithm to increase contrast of the low-contrast Images. Fig.7-9 (material suplementario) are the result after the different operation processing. We can observe a improvement of image quality at different method, and that the proposed operation can give effective result. In the image of histogram equalization processing, while the details of ray image are enhanced, the noise is increased, and the enhanced image has been enhanced. The details of Top-hat model are enhanced, and the image processed by wavelet method keeps the details of the image well, but there is noise in the edge area. The image processed by K-SVD model has been improved,the noise in the flat area is well removed, but the details are blurred at the same time.

The image was enhanced by using the histogram equalization method, but the background noise also increased. The image contrast was improved, but the gray level of the image decreased, and the details disappeared after being equalized. Table 1(material suplementario) indicated that the image suffered a serious loss in the details, and the contrast was affected after being processed due to excessive enhancement.

Laplace operator is a differential operator. This operator can be applied to strengthen the regions with gray mutation and weaken the ones with slow changes in grayscale. The original image was sharpened with a Laplace operator to generate an image with gray mutation. A sharpened image was then shaped through the superimposition between the Laplacian image and the original one. However, Laplace operator, which is isotropic, can enhance the image information and noise. Therefore, observations on the image processed by the Laplace operator confirmed that the details were enhanced, and noise was also increased in the X-ray images.

Figure 7-9(d) (material suplementario) is a sharpened image processed by wavelet transform. In the experiment, the image was decomposed into two layers. Artifacts appeared in the image and details were not enhanced. Wavelet transform decomposed the image into two parts: high frequency and low frequency. The image contour is mainly reflected in the low frequency part. The decomposition coefficients can be improved by decomposing the low frequency part. The high frequency decomposition coefficients are attenuated to achieve image enhancement. When traditional wavelet analysis is applied to industrial ray image processing, there is no difference between image details and contours, and the image contrast is low.

K-SVD is the most classical dictionary denoising algorithm. It can realize image processing by constructing a complete dictionary. Considering the running time and sample size, the dictionary is trained by 10 iterations in the experiment. The Figure 7-9(e) (material suplementario) is a sharpened image obtained by K-SVD. It can be seen from the graph that the image edge and details are blurred, and the image pairs are blurred. The image contrast is low.

The details of the processed image were not enhanced through Laplace algorithm, and the noise was increased. When Tophat algorithm was used, the details were enhanced to a certain extent, however, excessive enhancement was observed in the range line with evident white edge areas. The processed image was effectively enhanced through the proposed algorithm in this study, with enhanced X-ray image features, maintained flat area smoothness, and presence of suppressed artifacts.

This study conducted a comparative analysis from image contrast values to objectively evaluate the image quality. The proposed algorithm exerted enhanced advantages in protecting edge structural features. The images processed by the proposed models in this study obtained improvement in contrast, maintained a high structural consistency with the original ones, and retained abundant information.

## 5. CONCLUSIONS

With regard to low contrast and unclear details of industrial X-ray images, a sharpening method based on nonlocal differences was developed in this study on the basis of Laplacian sharpening model. The proposed method covered nonlocal features and structural similarity of images. The following conclusions could be drawn:

(1) Nonlocal means algorithm of filtering for images utilized the noncorrelation of noise and enlarged the search area of pixels in the neighborhood. With substantial similar pixels participating in the filtering process in the search window, this method was significantly effective in denoising.

(2) Images could be decomposed into structure and texture. Luminance, contrast, and structure were measured by the SSIM model to calculate the structural similarity, thereby strengthening the robustness of the aforementioned algorithm and reducing the computation time.

(3) The overall luminance of sharpening was controlled by parameter A in the high-enhancement sharpening mask. Images processed by mask that was analyzed with nonlocal differences were characterized with an enhanced transition, clear edge, and evident sharpening results.

The proposed algorithm in this study considers the denoising and edge preserving for weight vectors of visual words to accurately reflect the details of low-contrast images and offer convenient and accurate technical data for industrial X-ray detection. However, the adaptive selection for parameters of the algorithm when setting parameters should be further studied.

## REFERENCES

[1] Liu Dequan,Cui Tao, Yang Yaning. "Image Enhancement Based on Local Contrast Adaptive Histogram Equalization". China Computer & Communication. June 2016. Vol. 7. p.79-80.

[2] Xue Heru,Ma Shuoshi, Pei Xichun. "Color Image Segmentation Based on Mathematical Morphology and Fusion". Jounal of Image and Graphics. January 2017. Vol.11-12. p1764-1767.

[3] Zhao Cun, Hu Weiwei. "New algorithm for X-ray image enhancement". Transducer and Microsystem Technologies". June 2017. Vol.36-5.p.76-78.

[4] Liu Hui, Wan Wen, Xiong Zhenyu. "Defect detection and recognition technology of X ray weld image". Electric Welding Machine. June 2017. Vol. 47-4.p.89-93.

[5] Tian Yuan, Du Dong, Hou Runshi, Gao Zhiling. "Automatic inspection of weld defects using X-ray image sequences. Journal of TsingHua University(Science and Technology). September 2007. Vol.47-8.p.1278-1281.

[6] LIU Hui, WAN Wen, XIONG Zhenyu. "Defect Detection and Recognition Technology of X ray weld image". Electric Welding Machine. Aprail 2017. Vol. 47-4.p.89-93.

[7] Y. Li, X. Cao and J. Li. "A new cyber security risk evaluation method for oil

and gas SCADA based on factor state space". Chaos Solitons & Fractals. 2015. Vol. 89.p:203–209. https://doi.org/10.1016/j.chaos.2015.10.030.
[8] Wang Jiachen,Wang Xinfang. "Automatic Detection of Weld Defects in X-Ray Based on Background Image Reconstruction". Computer Systems & Applications.March 2018. Vol.27-2.p.245-249.
[9] Eckelt B, Meyendorf N, Morgner W, et al. "Use of automatic image processing for monitoring of welding processes and weld inspection". Non-Destructive Testing. April 1989. Vol.23-28. p.37-41. https://doi.org/10.1016/B978-0-444-87450-4.50012-6
[10] Anand R S, Kumar P. "Flaw detection in radiographic weld images using morphological approach". Ndt & E International. January 2006. Vol.39-1.p.29-33. https://doi.org/10.1016/j.ndteint.2005.05.005
[11] Daum W, Rose P, Heidt H, et al. "Automatic recognition of weld defects in x-ray inspection: British journal of nondestructive testing". Ndt & E International. March. 2003. Vol. 29-2. pp.79-81. https://doi.org/10.1016/0963-8695(92)90329-F
[12] Felisberto M K, Lopes H S, Centeno T M, et al. "An object detection and recognition system for weld bead extraction from digital radiographs". Computer Vision & Image Understanding. June. 2006. Vol.102-3.p.238-249. https://doi.org/10.1016/j.cviu.2006.02.004
[13] M Malarvel, G Sethumadhavan, PCR Bhagi, S Kar. "An improved version of Otsu's method for segmentation of weld defects on X-radiography images". Optik. August 2017.Vol.142.p.109-118. https://doi.org/10.1016/j.ijleo.2017.05.066
[14] YIN Ying, MAO Jian, SU Zhen-Wei. "PCA-Based Defect Enhancement and Segmentation for X-Ray Images of Welds".Nondestructive testing. September 2010. Vol.9.p.678-683.
[15] Chen Ming, MA Yuezhou, CHEN Guang. "Weld defects detection for X-ray linear array real-time imaging". Transactions of The China Welding Institution. July 2007. Vol.28-6.p.81-84.
[16] Zhang Xiaoguang, SUN Zheng, HU Xiaolei, HUAN Yuyue. "Extraction method of welding seam and defect in ray testing image". Transactions of The China Welding Institution. June 2011. Vol.32-2.p.77-80.
[17] Sun Yi, Sun Hongyu, Bai Peng, et al. "Real-time automatic detection of weld defects in X-ray images". Transactions of The China Welding Institution. June 2004. Vol. 25-2.p.115-118.
[18] J. Liu et al. "Discriminative feature representation to improve projection data inconsistency for low dose CT imaging".IEEE Trans. Med. Imag. December 2017. Vol.36-12. p.2499-2509.
[19] Chen Benzhi, Fang Zhihong, Xia Yong, Zhang Ling, Lan Shouren, Wang Lisheng. "Automatic detection of blowholes defects in X-ray images of thick steel pipes". Journal of Computer Applications. April 2017. Vol.37-3.p.849-853
[20] WANG Xin,GAO Weixin,WU Xiaomeng,WANG Zheng,LI Hua. "Image Detecting of Weld Defect Based on Fuzzy Pattern Recognition". Journal of Xi'an Shiyou University( Natural Science Edition). October 2016. Vol. 31-4.p.115-121.
[21] Shao Jiaxin, Dou Dong, Zhu Xinjie, GaoZhiling, Wang chen. "Defect Detection of Double-sided Weld Based on X-ray Digital Image Processing". Transactions of The China Welding Institution.February 2010. Vol. 31-11.p.21-24.
[22] M. Cesarelli, P. Bifulco, T. Cerciello, M. Romano, L. Paura. "X-ray fluoroscopy noise modeling for filter design". International Journal of Computer Assisted Radiology and Surgery. March 2013. Volume 8-2.p.269-278.
[23] T. Cerciello, P. Bifulco, M. Cesarelli, A. Fratini. "A comparison of denoising methods for X-ray fluoroscopic images". Biomedical Signal Processing and Control. November 2012. Vol.7-6.p.550-559. https://doi.org/10.1016/j.bspc.2012.06.004.
[24] L. Xiao, C. Li, Z. Wu, T. Wang. "An enhancement method for X-ray image via fuzzy noise removal and homomorphic filtering". Neurocomputing. June. 2016. Vol.195-26.p.56-64. https://doi.org/10.1016/j.neucom.2015.08.113.
[25] Y. G. Lee, J. Lee, Y. Shin, H. C. Kang. "Low-dose 2D X-ray angiography enhancement using 2-axis PCA for the preservation of blood-vessel region and noise minimization".Comput. Methods Progr. Biomed. January. 2016. Vol.123.p.15-26. https://doi.org/10.1016/j.cmpb.2015.09.011.
[26] S. Anand, R. S. S. Kumari. "Sharpening enhancement of computed tomography (ct) images using hyperbolic secant square filte". Optik. August.2013. Vol.124-15.p.2121-2124. https://doi.org/10.1016/j.ijleo.2012.06.026.
[27] S. Anand, R. S. S. Kumari, T. Thivya, S. Jeeva. "Sharpening enhancement of ultrasound images using contourlet transform". Optik. November. 2013. Vol.24-21.p.4789-4792. https://doi.org/10.1016/j.ijleo.2013.01.085.
[28] P. Bifulco, M. Cesarelli, T. Cerciello, M. Roman. "A continuous description of intervertebral motion by means of spline interpolation of kinematic data extracted by videofluoroscopy". J. Biomech. February. 2012. Vol.45-4.p.634-641. https://doi.org/10.1016/j.jbiomech.2011.12.022.
[29] G. Cao, Y. Zhao, R. Ni, A. Kot. "Unsharp masking sharpening detection via overshoot artifacts analysis". IEEE Signal Processing Letters. August. 2011. Vol. 18-10.p.603-606.
[30] Yang Guofeng. "Sub-arc X-ray welding defect image classifying algorithm". Chinese Journal of Scientific Instrument". August 2016. Vol.37-3.p.518-524
[31] Buades A, Coll B, Morel J M. "A Non-Local Algorithm for Image Denoising". IEEE. July. 2005. Vol. 2.p.60-65
[32] Yan-Li Liu, Jin Wang, Xi Chen, et al. "A Robust and Fast Non-local Means Algorithm for Image Denoising". Journal of Computer Science and Technology. February. 2008. Vol. 23-2.p.270-279.
[33] Chatterjee P, Milanfar P. "A generalization of non-local means via kernel regression". Proceedings of SPIE-The International Society for Optical Engineering. February. 2008. Vol. 6814-4.p.544-547. https://doi.org/10.1117/12.778615.
[34] Yi Zi-lin, Yin Dong, Hu An-zhou, Zhang Rong. "SAR Image Despeckling Based on Non-local Means Filter". Journal of Electronics & Information Technology, August 2012. Vol.4. p.950-955.
[35] Yang Xue-zhi, Chen Jing, Zhou Fang, Lang Wen-hui, Zheng Xin, Li Guo-qiang. "Polarimetric SAR Image Despeckling Using Non Local Means Filter Based on Homogeneous Pixels Preselection". Journal of Electronics & Information Technology, January 2016, Vol.37-12.p.2991-2999.
[36] SUN Weifeng DAI Yongshou. "Non-local Means Image Denoising with Multi-stage Residual Filtering". Journal of Electronics & Information Technology, August 2016. Vol.38-8.p.1999-2006.
[37] Zimmer S, Didas S, Weickert J. "Rotationally invariant similarity measures for nonlocal image denoising". Journal of Visual Communication and Image Representation. February. 2011. Vol.22-2. p.117-130. https://doi.org/10.1016/j.jvcir.2010.11.001
[38] Ji Z, Chen Q, Sun Q S, et al. "A moment-based nonlocal-means algorithm for image denoising". Information Processing Letters. November.2009.Vol.109-23.p.1238-1244. https://doi.org/10.1016/j.ipl.2009.09.007
[39] Li Qingzhong, Liu Qing. "Adaptive Enhancement Algorithm for Low Illumination Images Based on Wavelet Transform". CHINESE JOURNAL OF LASERS. February. 2015. Vol. 42-2.p.1-7.
[40] SUI Dan, JIAO Zhen, YANG Jie. "Image Enhancement Algorithm Based on Wavelet Analysis and Retine Algorithm". Journal of Jilin University (Science Edition). June. 2016. Vol.54-3.p.592-596.
[41] Dongwook Cho n, Tien D. Bui. "Fast image enhancement in compressed wavelet domain". Signal Processing. May.2014.Vol.98.p.295-307. https://doi.org/10.1016/j.sigpro.2013.11.007.
[42] Li Yang, Xinyu Geng and Haode. Liao, "A web sentiment analysis method on fuzzy clustering for mobile social media users", Eurasip Journal on Wireless Communications & Networking. 2016. Vol. 2016-1.p.1–13. https://doi.org/10.1186/s13638-016-0626-0.
[43] Yang Chen, Luyao Shi, Qianjing Feng, Jian Yang, Huazhong Shu, Limin Luo, Jean-Louis, Coatrieux, Wufan Chen. "Artifact suppressed dictionary learning for low-dose CT image processing". IEEE transactions on medical imaging. 2014. Vol.33-12.p.2271-92.
[44] Wang Z, Bovik A C, Sheikh H T, et al. "Image quality assessment: From error cisbility to structural similarity". IEEE Transactions on Image Processing. 2004. Vol.13-4.p.600-612.

## APPRECIATION

This study was funded by the National Key Scientific Instrument and Equipment Development Project of China under Grant 2014YQ24044508, in part by the National Natural Science Foundation of China under Grant 61671413, in part by the National Key Research and Development Program of China under Grant 2016YFC0101602, in part by the Shanxi Province Science Foundation for Youths under Grant 201801D221196.

## SUPPLEMENTARY MATERIAL

https://www.revistadyna.com/documentos/pdfs/_adic/9315-1.pdf